Deep-seated focused fluid migration as indicator for hydrocarbon leads in the East Shetland Platform, North Sea Province

Jens Karstens[1*], Philipp Müller[1], Christian Berndt[1], and Stefano Patruno[2]

[1]GEOMAR Helmholtz Centre for Ocean Research Kiel, Germany
[2]ONE-Dyas, London, U.K.
[*]jkarstens@geomar.de

ABSTRACT

Hydrocarbon exploration in the North Sea Basin has revealed a multitude of focused fluid conduits, which manifest in seismic data as pipe or chimney structures that in some instances are connected to underlying hydrocarbon reservoirs. 3D seismic data from the eastern margin of the East Shetland Platform (ESP) reveal the presence of more than 450 focused fluid conduits. Most of these initiate at the Base Tertiary Unconformity (BTU) and crosscut the overlying sediments. The focused fluid conduits correlate with intra-platform basin structures beneath the BTU and with permeable sediments lobes, channels and deltaic units in the overlying Paleocene to Eocene successions, which include known hydrocarbon reservoirs (e.g. Bressay, Bentley, Skipper or Piper). Clusters of pipes associated with other channels and deltaic units may indicate the presence of additional prospects at the eastern margin of the ESP. Our study highlights the potential of using seismically imaged focused fluid system analyses in hydrocarbon exploration in platform areas on both sides of the Viking Graben and other frontier areas as they reveal the presence of working hydrocarbon charge pathways.

1. INTRODUCTION

Hydrocarbon exploration in the North Sea Basin has revealed fluid flow features including pockmarks, gas accumulations and focused fluid conduits (Judd and Hovland, 2007). These structures often manifest in seismic data as vertically oriented amplitude anomalies known as seismic pipes and chimneys (see section 2.1; Berndt et al., 2005; Cartwright et al., 2007; Løseth et al., 2009). While pipe structures are generally associated with natural blowout-like fluid expulsion events (Løseth et al., 2011; Karstens and Berndt, 2015), seismic chimneys are interpreted as gas-filled fracture networks (Arntsen et al., 2007; Granli et al., 2007). Both types of fluid conduits form when overpressure within a formation exceeds the resistance of the cap rock against capillary or fracture failure (Hubbert and Willis, 1957; Clayton and Hay, 1994; Cathles et al., 2010). Thus, these structures are good indicators for past and present overpressure within sedimentary basins. Focused fluid conduits are often found above hydrocarbon fields in the North Sea. In particular, some focused fluid conduits are directly connected to fields (e.g. Tommeliten, Ekofisk; Arntsen et al., 2007; Granli et al., 1999). Therefore, focused fluid conduits have often been considered indicators for mature source rocks and potential hydrocarbon bearing reservoirs (Heggland et al., 2005; Løseth et al., 2009).

Because focused fluid conduits may indicate shallow over-pressured gas accumulation within the Cenozoic succession of the North Sea Basin, they are also important for drilling hazard assessment. Drilling through these intervals has resulted in uncontrollable blowout events including the West Vanguard (Norwegian Sea) blowout in 1985 and the 22/4B (British North Sea) blowout in 1990 (Ottesen et al., 2012; Leifer and Judd, 2015). These events highlight the importance of understanding shallow fluid flow systems, even when these are not connected to deep hydrocarbon reservoirs. Focused fluid conduits are also important for the long-term efficacy of subsurface storage (Karstens et al., 2017). For example, the geological storage of CO_2 as part of Carbon Capture and Storage (CCS) operations may become relevant in the future, as the North Sea Basin hosts the most suitable storage formations for industrial-scale implementation of this technology in Europe (Hazeldine, 2009).

The East Shetland Platform (ESP) is part of the UK Continental Shelf and lies west of the Viking Graben, north of the Witch Ground Graben and east of the Shetland and Orkney Islands (**Fig. 1**; Turner et al., 2018; Patruno et al., 2019; Scisciani et al., in press). Hydrocarbon exploration in the Central and Northern North Sea has mainly focused on areas overlying the mature Jurassic source rocks (e.g. Viking Graben, Central Graben, Moray Firth), while the ESP has received comparable little attention by hydrocarbon exploration. However, several discoveries on the ESP have proven the presence of heavy, but exploitable oil including the Mariner, Kraken, and Bressay fields (Patruno and Reid, 2016a). The discovery of the giant Johann Sverdrup field on the Utsira High, which represents the conjugate platform and is separated from the ESP by the South Viking Graben, spiked new commercial interest in the platform areas on all sides of the major upper Jurassic graben.

This study focuses on the analysis of focused fluid manifestations and their relation to potential deep lying source rocks and hydrocarbon plays in the ESP. Our first objective is to compile an inventory of vertically-oriented seismic amplitude anomalies in four dual-sensor broadband 3D seismic surveys acquired by PGS in 2011-2015, covering 3800 km^2 of the eastern margin of the ESP. The analysis of focused fluid flow structures has proven to represent an effective tool to reconstruct the timing and controls fluid expulsion and overpressure accumulation during the evolution in the North Sea Basin and to detect hydraulic connections between the deep subsurface and the seafloor (Karstens and Berndt, 2015; Karstens et al., 2018; Böttner et al., 2019). We have analysed the seismic anomalies and differentiate between anomalies that are seismic imaging artefacts and structures associated with focused fluid migration. The stratigraphy of the study area is subdivided in a shallow and a deep succession by a major unconformity (Base Tertiary Unconformity; see section 2.2). The second objective is to correlate the spatial distribution of fluid flow manifestations with structural elements beneath this unconformity. The third objective is to identify the structural and depositional elements controlling the refocusing of fluid flow above the unconformity. We have analysed the influence of permeability contrasts on the accumulation of overpressure and focusing of fluid migration. The fourth objective is to analyse the spatial correlation between focused fluid conduits and known hydrocarbon reservoirs to improve our understanding of potential plays in the East Shetland Platform.

2. GEOLOGICAL BACKGROUND

2.1. Focused fluid conduits in seismic data

The presence of free-gas in the pore-space of marine sediments has a strong impact on seismic waves travelling through marine sediments (White, 1975) leading to a disturbed seismic appearance, as well as amplitude and velocity anomalies in seismic data (Granli et al., 1999). Seismic anomaly observations associated with subsurface fluid flow and gas accumulations include bright and dim spots, phase reversals, and push-down or pull-up of seismic reflections (Løseth et al. 2009). Vertically-oriented seismic anomalies characterized by one or several of these observations have been termed seismic pipes or chimneys (Berndt et al., 2005; Cartwright et al., 2007; Løseth et al., 2009; Andresen, 2012; Karstens and Berndt, 2015; Cartwright and Santamarina, 2015). There is some confusion in the literature regarding the use of the terms seismic pipes or chimneys. Here, we use the classification of Karstens and Berndt (2015). The term seismic chimney (elsewhere called gas chimney or gas cloud) originally described dimmed or wiped-out zones, which had been identified in seismic data above several hydrocarbon fields in the North Sea, e.g. Ekofisk (Hovland and Sommervile, 1985), Hild (Lønøy et al., 1986), and Tommeliten (Granli et al., 1999). Shear-wave experiments, seismic modelling, and wellbore data indicate that the Tommeliten seismic chimney represents a gas-filled fracture network (Granli et al., 1999; Arntsen et al. 2007). Chimney structures have diameters of several kilometres and their boundaries are not necessarily straight vertical lines, which distinguishes them from seismic pipes, which are characterized by bended and broken reflections, bright spots, and a comparably narrow diameter and largely vertical edges, e.g. Nyegga (Plaza-Faverola et al., 2011; Karstens et al., 2018), offshore Angola (Løseth et al., 2011), or the Danube delta (Hillman et al., 2017). Seismic pipes are interpreted as an analogue to natural blowout events and attributed to the rapid release of over-pressured fluids (Moss and Cartwright, 2010; Løseth et al. 2011; Karstens and Berndt, 2015). Both, seismic pipes and chimneys have been analysed in the context of seal bypass systems (Cartwright et al., 2007), hydrocarbon leakage systems (Løseth et al., 2009), and hydrocarbon plumbing systems (Andresen, 2012) and it has been concluded that they are indicators for the transport of fluids and overpressure between different reservoirs by focused fluid flow.

Seismic acquisition geometry of conventional 3D seismic surveys is good at imaging horizontal or gently dipping reflectors in the subsurface, but it is less conducive to in imaging vertically-oriented structures such as focused fluid conduits. Fluid flow is often associated with gas accumulations causing high amplitude reflections, which impede the seismic imaging of underlying structures due to the loss of seismic energy or scattering. The presence of gas significantly affects seismic velocities and caused imperfect imaging if lateral and vertical velocity heterogeneities are not resolved during processing. All these effects may as well manifest as vertical oriented seismic anomalies and need careful consideration, when distinguishing between focused fluid conduits and seismic artefacts (Karstens and Berndt, 2015).

2.2. <u>Development of the East Shetland Platform</u>

The ESP is located west of the Viking Graben and north of the Witch Ground Graben, which represent two branches of the Late Jurassic to Early Cretaceous rift system that formed the North Sea Basin (**Fig. 1**; Ziegler et al., 1992; Turner et al., 2018). The transition from the active rifting phase to post-rift thermal subsidence is manifested by the 'Late Cimmerian Unconformity' (Badley et al., 1988; Gabrielsen et al., 1990; Nøttvedt et al. 1995), also known as the 'Base Cretaceous Unconformity', which is typically buried by the up to 3 km thick Kimmeridge Clay in the graben systems (Ziegler, 1975a,b; Johnson, 1975; Fyfe et al., 1981; Rawson and Riley, 1982) This unconformity eroded into the whole Northern North Sea and is the most prominent reference horizon in the seismic data and wireline logs (Rønnevik et al., 1975; Gabrielsen et al., 1984, 1990; Blystad, et al., 1995). However, this unconformity is diachronous and includes several regional as well as locally limited unconformities, which have been eroded in Late Jurassic to Early Tertiary times (Rawson and Riley 1982, Brown 1990; Hancock 1990; Davies et al.1999; Turner et al., 2018). Therefore, Kyrkjebø et al. (2004) introduced the term 'Northern North Sea Unconformity Complex' to integrate these unconformities. Especially outer platform areas such as the ESP have been affected by multiple episodes of erosion due to their exposed position and complex geological evolution (Kyrkjebø et al., 2004). For simplicity, we will refer to this unconformity as the Base Tertiary Unconformity or BTU.

The eastern part of the ESP was uplifted during the Aalenian Doming in the Early to Middle Jurassic and the Alpine compression and inversion episodes in the Late Cretaceous to Eocene (Underhill and Partington, 1993; Patruno and Reid 2016a, 2017). This uplift was superposed onto the long-term post rifting thermal subsidence since the Early Cretaceous. These events are manifest in the stratigraphic sequence with missing Lower – Middle Jurassic deposits, very thin and local veneers of Bathonian (Middle Jurassic) to Lower Cretaceous rocks, and Upper Cretaceous Chalk Group limestones and marlstones varying locally in thickness from very thin veneers to up to several hundred meters thickness (Patruno and Reid, 2017; Patruno et al., 2019). Since the Eocene, the uplift of the British Isles and subsidence in the Central North Sea and South Viking Graben caused westward tilting of the ESP (Patruno and Helland-Hansen, 2018; Patruno et al., 2019; Scisciani et al., in press). Regional and global sea-level fluctuations during the Cenozoic and Early Pleistocene resulted in the deposition of alternating sequences of clay-rich units deposited during sea-level rise and high-stands and sand-rich, deltaic units deposited during sea-level fall and low-stands (Patruno and Helland-Hansen, 2018; Patruno et al., in press). These were locally incised by channel erosion during sea-level low-stands (Underhill, 2001). During the Middle and Late Pleistocene, the North Sea Basin was repeatedly covered by thick ice-sheets leading to the deposition of alternating layers of glacigenic tills and glaciomarine sediments (Ottesen et al., 2014; Reinardy et al., 2017; Sejrup et al., 2018; Patruno et al., in press). The glacially affected sediments were reworked by ice-stream activity and subglacial tunnel valley formation (Graham et al., 2011; Stewart & Lonergan, 2011; Reinardy et al., 2017) and formed several glacial unconformities.

2.3. Source rocks for hydrocarbon reservoirs in the ESP

The primary source rock for most hydrocarbon reservoirs in the Central North Sea is the Late Jurassic Kimmmeridge Clay, which reached the oil and gas window in the Jurassic aged graben systems in the Central North Sea (e.g. Pegum and Spencer, 1990; IGI, 2017). In the ESP, the Kimmeridge Clay is absent or thin (<10-50 m) and thermally immature (Patruno and Reid, 2016a; IGI, 2017). However, the geochemical signature of some hydrocarbon discoveries in the ESP (e.g. Mariner and Kraken Fields) suggest that these were charged by the Kimmeridge Clay via lateral migration of up to 30 km from the Viking Graben (Fig. 1; IGI, 2017). Additionally, Permo-Triassic intra-platform mini-basins may contain a Middle Devonian source rock (e.g., Duncan and Buxton, 1995; Patruno and Reid, 2016a, b, 2017; Patruno et al., 2018, 2019; IGI, 2017).

In particular, Middle Devonian organic-rich lacustrine sediments of the Orcadia and Eday Flagstone formations, reached a mature to post-mature state according to vitrinite reflection analysis of core material (e.g. well 9/16-3, Duncan and Buxton, 1995; Marshall and Hewett, 2003). This is in agreement with 1D basin modelling, which revealed that the Middle Devonian in the Permo-Triassic intra-platform mini basins are mature in large areas of the ESP (Patruno and Reid 2016a; 2017; Patruno et al., 2018; IGI, 2017). In addition, geochemical constraints indicate that the Jurassic-age reservoir of the Beatrice Field was charged with Devonian aged hydrocarbons (Duncan and Buxton 1995; Marshall and Hewett, 2003). Although primarily sourced by the Kimmeridge Clay, Devonian aged hydrocarbons contributed to the charging of several large fields in the Witch Ground Graben (e.g. Claymore, Piper, Tartan, and Buchan Field; Marshall, 1998; Cornford, 2009; Monaghan et al., 2016) and West of Shetlands (e.g. the Clair Field; Mark et al., 2008).

The ESP includes several potential reservoir units including sediments of Early Eocene to Devonian age. These include shelfal clinoforms (e.g. Bentley discovery) and sandy channel fills (e.g. Bressay discovery) of the Upper Paleocene to Lower Eocene (Pegrum and Spencer, 1990; Underhill, 2001; Patruno et al., 2015) as well as Lower and Middle Paleocene deep marine sandstones forming stratigraphic and or structural traps (e.g. Kraken and Mariner Field; Patruno et al. 2018). Further potential reservoir units are thin Upper Jurassic sandstone veneers, which form structural and pinch-out traps (e.g. Piper Field; Maher 1981), and structural traps in Permo-Triassic intra-platform sandstones and Zechstein carbonates (e.g. Crawford discovery and Claymore field; Yaliz, 1991; Harker et al., 1991; Whitehead and Pinnock et al., 1991). In addition, there are Rotliegend sandstones, weathered and fractured crystalline basement along the platform margin (e.g Cairngorm discovery; UKCS Licences P1214 and P1892, Blocks 16/2b and 16/3d) as well as large fractured Devonian sandstones that all form structural traps in the ESP (e.g. Buchan Field; Hill and Smith, 1979).

3. DATA AND METHODS

This study is based on the analyses of four 3D seismic datasets, i.e. PGS14003, PGS15004, PGS15010-01, and PGS15010-02, which were acquired using towed dual sensor broadband (GeoStreamer) by PGS between 2011 and 2015 (**Fig. 1**). The four datasets have a bin size of 12.5 m and cover a total area of ~3,800 km^2. The vertical resolution ($\lambda/4$) is about 18 to 23 m at the level of the BTU and decreases to values greater than 50 m beneath the BTU. More details on the acquisition and processing parameters are shown in **Tab. 1**.

In addition, we integrated publically available data and interpretations from exploration wells provided by the UK Oil and Gas Authority, which includes check shots, well paths, well logs, and various reports (**Fig. 1**).

The seismic data analysis included mapping of vertically oriented seismic anomalies in all four seismic cubes. Building on this catalogue, we distinguished between seismic anomalies, which are likely seismic manifestations of fluid flow structures (seismic pipes) and seismic anomalies caused by imaging or processing artefacts. Within the catalogue of anomalies classified as focused fluid conduits, we distinguished between single pipe structures and clusters of pipes. Those anomalies classified as fluid flow-related were further analysed regarding their evolution in a structural and depositional context. Finally, we investigated the spatial correlation between fluid flow in the shallow subsurface and deep structural elements by 3D seismic interpretation of seismic horizons and 3D seismic attributes.

4. RESULTS

4.1. Seismic stratigraphy and focused fluid manifestations

The four analysed datasets are located at the eastern margin of the ESP. Dataset A and the north of B cover the transition from the ESP into the Viking Graben (Beryl Embayment) towards the east, while datasets C and D are located entirely on platform areas (**Fig. 1**). The most prominent reflection in all datasets is the BTU (**Figs. 2 and 3**), which in the platform areas is characterized by high amplitudes due to the direct contact between less lithified Cenozoic strata with more lithified Paleozoic rocks. In dataset A, the BTU reflection deepens from about 0.7 seconds two-way-travel time (s TWT) in the west to about 2.1 s TWT in the east and follows three major fault blocks (**Fig 2A**). The seismic data beneath the BTU of the western and central block show only few resolvable structures, while the eastern block overlies a wedge of sediments pinching out on top of the seismic basement. Several pipe structures initiate at the BTU, where they coincide with areas with dimmed seismic amplitudes or the edge of fault blocks (**Fig. 2A**). The Paleogene to Neogene successions overlie the BTU and consist of well-stratified, eastward-dipping sediments that are locally affected by polygonal faulting. The pipe structures either terminate within these sediments or at an unconformity characterized by seafloor-parallel sediments and v-shaped reflections indicating erosional channels.

In dataset B, the BTU overlies platform areas and only the northeastern part of the cube covers the transition to the Viking Graben (**Fig. 1**). The stratigraphy beneath the BTU is dominated by a Devonian syncline (Patruno et al. 2019, Scisciani et al. in press), whose steeply inclined strata are imaged by the seismic data (**Fig. 2B**). Several pipe structures correlate spatially with the interception of the syncline and the BTU (**Fig. 2B**). The Paleocene succession overlying the BTU and includes several channel structures, which are crosscut by pipe structures. In some places pipe structures originate from these channels. The Paleocene succession also contains the prograding Dornoch delta (Underhill, 2001; Patruno and Helland-Hansen, 2018) that pinches out towards the east. The Paleocene to Neogene sediments consist mainly of bedding-parallel units and the boundary to Quaternary sediments is difficult to constrain.

Dataset C covers only platform areas and the BTU overlies several basin-structures (**Fig. 1**). These structures are less pronounced than in dataset B but consist also of steeply inclined strata, which are part of the Crawford-Skipper Basin and Upper-Permian basins shown by Patruno and Reid (2017; **Fig. 3A**). The Paleocene to Neogene successions consist of alternating sequences of deltaic and bedding-parallel units intersected by several channel structures. These sediments are crosscut by several pipe structures, which origin at the BTU or at channel structures (**Fig. 3A**). Close to the seafloor, channel structures have eroded deeply into the underlying sediments marking the Quaternary unconformity.

Dataset D is located at the southern margin of the ESP (Piper Shelf) close to the Witch Ground Graben to the south (**Fig. 1**). The BTU is well developed and overlies strongly deformed strata, which dip towards the west (**Fig. 3B**). These correspond to the intra-platform Permian and Jurassic basin fills described by Patruno et al. (2019; in particular their figures 15C-D and 22B). The Paleocene succession consists of a well-developed prograding deltaic unit belonging to the Dornoch Formation, which overlies a channel structure in the west. In the east the Paleocene sediments include several saucer-shaped structures with high seismic amplitudes. They crosscut the strata and are overlain by mound structures (**Fig. 3B**). The Neogene-Eocene succession consists of prograding deltaic and bedding-parallel units and is in areas incised deeply by channel structures, which mark the Quaternary unconformity. Pipe structures initiate either at the BTU, at the top of prograding deltaic units or at the edges of the saucer-shaped structures.

The four datasets image many seismic pipe and chimney structures, which occur as singular features or in clusters (**Figs. 2-4**). These vertically oriented seismic anomalies are often characterized by upward-bended reflections and bright spots. Most of the pipe structures initiate at the BTU reflection and terminate at various levels beneath the seafloor; none of the structures reach the seafloor. We have mapped 87 vertically oriented seismic anomalies in dataset A, 256 in dataset B, 181 in dataset C and 40 in dataset D. Many of them are associated with increased seismic amplitudes (**Figs. 2-4**).

5. <u>DISCUSSION</u>

5.1. Focused fluid conduit inventory

In total, we have mapped 564 vertical seismic anomalies cross-cutting the sediments above the BTU. Not all of these represent focused fluid conduits, but some are the result of imaging or processing artefacts. Common examples for seismic artefacts in the datasets are stacks of upward bended seismic reflections found beneath the apex of tunnel valleys (**Fig. 5A, B**). Such stacks of upward bended seismic reflections are the result of velocity heterogeneities within the valley infill, which have not been resolved in the seismic velocity model during processing (Kristensen and Huuse, 2012). However, some vertical seismic anomalies beneath tunnel valleys include additional seismic features such as broken reflections or bright spots, which cannot be explained solely by velocity heterogeneities in the overburden, and possibly represent real geological features (Hseinat and Hübscher, 2014; Karstens and Berndt, 2015).

The vertical seismic anomalies beneath tunnel valleys in the analysed datasets generally lack amplitude variations and, thus, most likely represent imaging artefacts. Some seismic anomalies beneath tunnel valley infills follow the extent of the overlying tunnel valley over several km (Fig. 5D), while others have a circular shape and are more difficult to classify as seismic artefact. Another type of vertically-oriented seismic anomalies representing imaging artefacts is frequently observed beneath high amplitude bright spots (**Fig. 5C**). These anomalies dim the underlying reflections and often lead to pull-ups of reflections and a distorted seismic appearance. These effects often decrease with depth as more seismic energy undershoots the bright spot. While the identification of these types of anomalies as seismic artefacts is comparably easy, the classification of anomalies with narrow diameter and limited vertical extent can be highly ambiguous. Where these features correlate with structural heterogeneities in the overburden, we also classified them as seismic artefacts. In total, we classified 108 of the 564 anomalies as seismic artefacts and 456 as focused fluid conduits. These focused fluid conduits are grouped into 65 clusters of focused fluid conduits consisting of 352 pipe structures and 104 singular fluid conduits.

5.2. **Sources of migrating fluids**

The study area extends about 250 km north to south and the analysed dataset covers about 50% of the eastern margin of the ESP. In this area, several hydrocarbon reservoirs have been discovered (e.g. Kraken Field, Bressay Field), but it represents a yet-underexplored area in the North Sea Province. The current understanding is that hydrocarbon fields (mainly containing heavy oils at present day) in the ESP have been charged via lateral migration along permeable beds in the Paleocene succession sourced by mature Kimmeridge Clay of the Viking Graben. Our focused fluid flow analysis reveals that many focused fluid conduits in the analysed datasets can be traced down to the BTU, suggesting either lateral migration through a permeable bed just above the BTU or direct vertical rise of thermogenic hydrocarbons from the pre-Cretaceous successions. In dataset A, the BTU is affected by pronounced faulting due to rifting of the Viking Graben. There is no spatial correlation between focused fluid conduits and the boundary of the ESP and the fault blocks of the Viking Graben (**Figs. 2**). To the contrary, focused fluid conduits in the northernmost seismic dataset generally initiate in the centre of the fault blocks rather than at their boundaries and form an east west oriented band of singular and clustered pipe structures (**Fig. 6A**). The easternmost pipe cluster originates in the eastward-dipping Upper Jurassic source sediments, which have reached the oil-window further to the south (Patruno and Reid, 2017). Due to buoyancy hydrocarbons may have migrated along tilted permeable layers towards the west and fuelled the easternmost pipe cluster. The pipe clusters further west initiate mainly at the BTU and thus have either been charged by deeper source rocks or relied on a deeper (just above the BTU) carrier bed for lateral migration.

Towards the south, datasets B and C cover the eastern margin of the ESP, while the boundary to the Viking Graben (Beryl Embayment) is covered in the northeastern corner of dataset B. There are some seismic anomalies above the transition between these two structural provinces, which will be discussed in section 5.4 (**Fig. 6B**). Dataset B and C include a large number of singular and clustered seismic pipe structures (**Figs. 6B and 7A**). These pipes initiate mainly at the BTU and they often correlate spatially with the Permo-Triassic intra-platform mini-basins (e.g. the edges of the Crawford-Skipper Basin – Patruno and Reid, 2017; Patruno et al., 2019). In datasets B and C, fluid conduits initiate preferentially in the centre and at the margins of these deep basins (**Figs. 2 and 3**). The Devonian basin in dataset B is subdivided into two mini-basins by an inverted Devonian extensional master-fault (**Figs. 6B and 8;** Patruno and Reid 2017; Patruno et al., 2019; Scisciani et al., in press). The sub-BTU Paleozoic intra-platform depocentres in dataset C have a more complex structure and are collectively known as the Crawford Skipper Basin. Evidence of mature Devonian source rocks exists for the edge of the Crawford-Skipper Basin (Well 9/16-3; Duncan and Buxton, 1995; Patruno et al., 2019; Patruno and Reid, 2017), while possibly mature oil-prone Carboniferous source rocks are present in Quadrant 15, in parts of the Piper Shelf and the Dutch Bank Basin (e.g., IGI, 2017). The Crawford Skipper Basin is subdivided into discrete structural depocentres by a prominent fault structure (**Fig. 7A**). The deep basement faults in datasets B and C correlate with overlying hydrocarbon fields (**Fig. 8**). The extent of the Kraken Field mimics the trace of the underlying inverted extensional master-fault in dataset B, while the leads in dataset C cluster around an underlying basement fault structure. The spatial correlation between Paleocene discoveries and structural elements of underlying intra-platform basins may indicate hydrocarbon migration from Devonian and Permo-Triassic source rocks into these reservoirs, which represents a charging mechanisms alternative to the commonly assumed lateral hydrocarbon migrations from the Viking Graben (Beryl Embayment). The charging mechanism cannot be determined solely based on seismic data and requires additional geochemical constraints. Numerical basin simulations indicated that putative Middle Devonian source rocks in the mini basins have reached the oil window (Patruno and Reid 2016a; 2017).

Dataset D is located at the southern margin of the ESP and shows only few pipe structures, which cluster around the margins of a basin structure (**Fig. 7B**). A second prominent focused fluid flow structure is located at a saucer-shaped reflection further east (**Fig. 3B**) that we interpret as a sand injection because it edges show characteristic wing-structures (Huuse et al.

2004; Szarawarska et al. 2010). Subtle bright spots occur between the BTU and the sand injection and may indicate that over-pressured fluids from pre-Cretaceous successions have led to sediment mobilization and focused fluid flow (**Fig. 3B**).

5.3. Refocusing of fluids in Paleogene sediments

While most pipe structures in all four datasets are perfectly vertical and reach from the BTU to the shallow subsurface, other fluid conduits are more complex and indicate refocusing of fluids and overpressure in specific tectono-stratigraphic units. The sand injection in dataset D is a prominent example of refocusing of upward migrating fluids. The edges of the sand injection correlate spatially with stacks of bright spots indicating the presence of free gas in multiple layers above the injection complex (**Fig. 3B and 9A**; Løseth et al., 2009). The formation of sand injection is generally associated with the increase of pore pressure in unconsolidated sand layers or bodies, which then breach the overlying caprock and intrude into the overlying strata (Huuse et al. 2004; Szarawarska et al. 2010). The gas accumulations above the wing-structure of the sand injection may either indicate that the injected sand-pore fluid mixture had a high gas content or that the sand injection allowed gas to migrate into the injected sand body afterwards. Either way, the highly permeable sand injection affected the distribution of deep-rooting fluids in the overburden by refocusing.

Refocusing of fluids can also be observed in dataset A, where fluid conduits ascending from the BTU change appearance after crossing a seismic horizon characterized by patches of high amplitude reflections (marked pink in **Figs. 2A and 9B**). The seismic amplitude map of this horizon indicates several northeast to southwest oriented slightly meandering lobes characterized by high amplitudes (**Fig. 9B**). Areas with focused fluid flow show generally lower seismic amplitudes. The lobe-like structures are not visible as distinctive tectono-stratigraphic features (e.g. channels, clinoforms) in seismic profiles indicating these structures must be thin relative to the seismic resolution. The changes in seismic amplitude in relation to the presence of focused fluid conduits indicate that fluid migration has an impact on the acoustic impedance, which are most likely caused by variable gas content. The observation of conduits terminating at this horizon indicates that ascending over-pressured gas has been able to migrate and charge this formation, which indicates a high permeability in comparison to the surrounding strata (Karstens and Berndt, 2015).

We interpret the lobe structures as sand-rich channel deposits, although they are much thinner than deeper buried systems, which are present in dataset B and C. Several pipe structures crosscut these channel systems, which locally show patches of increased amplitudes in the Paleocene succession (**Figs. 2B, 3A and 9C**). The channel systems formed during sea level low-stands, are filled with sand-rich deposits and were covered by finer-grained deposits (Underhill, 2001). One prominent example is the channel system in dataset B (**Lead 2 in Fig. 2B**), which consist of channel deposits, which have been deposited parallel to the paleo-shoreline and are gas- and oil-bearing (**Fig. 3A**; Underhill, 2001). Fluid conduits affecting these channel systems are either originating at its top or crosscut the channel deposits indicating a hydraulic connection to sub-BTU sediments. The channel systems distribute hydrocarbons from localised spill points over a large area. Another prominent example for such fluid redistribution is the Lista Channel in dataset C (**Fig. 3A**). The Lista Channel has been drilled by exploration well 8/20-1, which revealed high sand content in the channel deposits sealed by fine-grained sediments above. Several pipe structures initiate from the Lista Channel indicating that it may as well act as a distributor for deep-sourced fluids (**Fig. 9C**). More channel systems overlie the Lista Channel, representing several sand-rich intervals (**Fig. 7A**) and exploration wells (e.g. 9/21-1) revealed oil in the pore space indicating upward migration of mature hydrocarbons from deeper reservoirs.

Sea level fluctuations in the Paleocene and Eocene have caused deposition of prograding deltaic clinoforms (Dornoch Formation – c.f., Patruno & Helland-Hansen, 2018), which are present in datasets B, C and D. These deposits are associated with prominent clusters of bright spots and pipe structures (**Figs. 2B, 3B, 6B, 7 and 9D).** However, pipe structures initiating from these deltaic units are often less pronounced and their spatial distribution is less focused compared to those associated with the Paleocene channel systems.

5.4. Implication of focused fluid flow for potential hydrocarbon plays in the East Shetland Platform

Analysis of the distribution of pipe structures in the ESP shows that most of these structures correlate spatially with mature Permo-Triassic intra-platform mini-basins beneath the BTU (e.g. Crawford Skipper Basin), highly permeable stratigraphic features in the Paleogene to Neogene or a combination of these. The spatial correlation between pipe structures and hydrocarbon reservoirs and discoveries is most striking. Dataset B comprises three major hydrocarbon fields including the Kraken Field, the Bressay Field and the Bentley field. The

Bressay Field is limited by a branch of a Paleocene channel system and contains estimated recoverable reserves of 100-300 million barrels of oil according to its operator Equinor. The Bressay Field correlates strongly with focused fluid conduits, which delineate its location almost perfectly (**Fig. 6B**). The Bentley Field is located in coarse-grained subunit of the Dornoch delta (Underhill, 2001) and contains up to 267 million barrels of recoverable heavy oil (according to its operator Xcite Energy). The pipe structures are clustering in the northern half of the reservoir. The Kraken Field reservoir is located in the Paleocene succession (Patruno and Reid, 2017) holding more than 400 million barrels of recoverable oil (according to its operator Enquest). The Kraken reservoir is located on top of an inverted Devonian master fault cutting through the local mini-basin structure and is not related to any prominent pipe structure. Assuming charging from either below or from lateral migration from Kimmeridge Clay source rocks in the Viking Graben (Beryl Embayment), the lack of pipe structures may be explained by fluid migration along the fault inhibiting the accumulation of high pore overpressure at the BTU, which would be required to form pipe structures.

Dataset C is located just south of the Mariner Field and covers the Crawford Skipper Basin, which is subdivided by a fault, whose location correlates with the Paleocene Selkie and Kelpie prospects and the Skipper discovery (**Fig. 7A**; Relinquishment Report for License P976). These hydrocarbon fields and prospects correlate with pipe structures. Dataset D partly covers the Piper oil field as well as the Brooks discovery and the Zeta prospect (**Fig. 7B**; relinquishment report for seaward production licence P1946). The focused fluid conduits in dataset D correlate spatially with the edges of hydrocarbon reservoirs (northern tip of the Piper reservoir and southern edge of the Zeta prospect; **Fig. 7B**) and escaping fluids from these reservoirs are the likely source of the observed focused fluid migration.

The strong spatial correlation between hydrocarbon reservoirs and focused fluid conduits reveals that in particular clusters of pipe structures represent a valuable indicator for the presence of migrating hydrocarbons in the ESP. Seismic datasets B and C contain additional pipe clusters, which originate from or terminate in stratigraphic features (e.g. channels or deltaic units) that show similarities to proven reservoirs in the area (**Figs. 6, 7 and 10**). One of these potential leads is located in the northern half of dataset B at the boundary to the Viking Graben (Lead 1 in **Figs. 2B, 6B and 10B**). A seismic amplitude map of the BTU horizon reveals patches of high amplitudes, which correspond to these structural highs (**Fig. 10A, B**). A cluster of pipes originates next to the strongest amplitude anomaly, which forms a stratigraphic trap above a wedge of Jurassic sediments (Lead 1; **Figs. 2A, 6B, 10A, B**). The amplitude anomaly above the wedge of Jurassic sediments stretches from the pipe cluster above the slightly dipping Jurassic unit towards the southeast, where it becomes patchier and less pronounced. The structurally controlled amplitude anomaly in combination with the pronounced pipe structures originating from the BTU are strong indicators that hydrocarbons have migrated up-dip along the Jurassic sediments and may have formed a reservoir that is similar to the Hood Field (Patruno and Reid, 2017).

An example for another type of lead is located in direct vicinity of the BTU amplitude anomaly, where multiple pipe structures connect the boundary of the Jurassic sediment wedge (related to Lead 1) and the Devonian basin with a channel structure (Lead 2 in **Figs. 2B, 10A**). This channel structure represents one branch of the channel system, which holds the Bressay reservoir (Lead 2 in **Fig. 6B**; Underhill, 2001). Both channel branches are strongly affected by focused fluid migration from beneath. The Jurassic sediment wedge and the Devonian basin represent two potential hydrocarbon sources for the northern branch of the channel, which may thus represent a lead similar to the neighbouring Bressay reservoir. Similar channel-bound plays are present in dataset C (Lead 4 and 5 in **Figs. 3A; 7A**) and dataset D (Lead 6 in **Fig. 7B**). The Lista Channel in dataset B shows similarities to the Bressay channel system and multiple pipe structures indicate the paleo migration of hydrocarbons (**Fig. 8C**). The Lista channel contains several amplitude anomalies and may have acted as pathways for hydrocarbons for the Skipper Field (**Figs. 8A, 9C**).

The third type of potential prospect is linked to deltaic units similar to the Bentley reservoir (Dornoch Formation), which are present in datasets C and D (**Figs. 3, 7, 10C and D**). In dataset C, several leads can be identified at the western end of the Lista Channel (**Fig. 7A**). These are linked to the channel itself (Skipper reservoir; Patruno and Reid, 2017) and the overlying Dornoch Formation (e.g. Kelpie prospects; Relinquishment Report for License P976), which are located within the Paleocene succession. However, several pipe structures by-pass the Paleocene sediments and terminate in an overlying deltaic unit. This deltaic unit includes several patchy amplitude anomalies within Eocene Horda Fomation, which follow the western boundary of this unit (Lead 3 in **Fig. 7a and Fig. 10C-D**). The patchy high amplitudes have a similar appearance as the anomalies of the Bentley reservoir and are limited to the outer boundary of a deltaic unit (Dornoch Delta in **Figs. 6B**).

These potential leads in combination with the known reservoirs highlight that focused fluid conduits are a useful indicator for hydrocarbon plays on the ESP. High permeable channel and prograding deltaic units are the most important controls of deep-sourced hydrocarbon migration above the BTU and at the same time represent important reservoir rocks. The presence of pipe structures cutting through or ascending from these units indicates that over-pressured fluids, especially gas, may have already escaped these reservoirs. However, it remains unclear if the leakage included light oil as well and thus only heavy oils (comparable to known hydrocarbon field in the ESP) are left. The formation of pipe structures may potentially have destroyed the seal of previously promising prospects (e.g. the Selkie prospect in cube C, where the discovery well 8/25a was dry (Relinquishment Report for License P976). However, even if lighter hydrocarbons have left such primary reservoirs, they may have accumulated in shallower stratigraphic units in e.g., Oligocene-Neogene sands (e.g. Lead 3).

6. CONCLUSIONS

The ESP represents one of the least explored areas of the North Sea Basin, but hosts several mainly Paleocene hydrocarbon discoveries (e.g. Kraken Field, Bressay Field, Bentley Field or Skipper discovery). The analysis of four 3D seismic datasets from the ESP reveals the presence of more than 550 vertical seismic anomalies. About 100 of these could be classified as seismic artefacts and more than 450 as seismic pipe structures associated with focused migration of fluids. Most of these structures originate from the BTU and correlate with intra-platform Paleozoic and Triassic basins, which may contain Middle Devonian and/or Carboniferous source rocks (**Fig. 11**). Recent geochemical analysis of core samples and numerical simulations indicate that these source rocks are thermally mature and may represent an additional contributor for charging Paleogene hydrocarbon reservoirs in the ESP. While lateral migration from the Kimmeridge Clay source rocks in the Viking Graben to the west represents the accepted primary charging mechanism for reservoirs on the eastern margin of the ESP, the pipe structures suggest (at least a secondary) additional thermogenic hydrocarbon source in the ESP. This source may be of particular interest in the Piper Basin and Dutch Bank Basin areas, which are out of reach from the lateral migration from the Viking Graben. Other pipes originate from Paleogene channels and prograding units, which represent reservoirs for deeply sourced hydrocarbons. Many pipe structures in the ESP correlate spatially with proven hydrocarbon fields and identifiable seismic leads (e.g., amplitude anomalies). In addition to these known hydrocarbon plays, the distribution of pipe structures indicates several potential plays in the Cenozoic succession of the ESP, which may be of commercial interest and represent targets for future hydrocarbon exploration at the ESP. On the other hand, the presence of pipe structures may be an indicator for the escape of light hydrocarbons (gas and light oil) from previously valuable reservoirs (e.g., Jurassic and Paleogene), and their possible migration into shallower targets, which have been typically overlooked by exploration (e.g., Oligocene-Neogene sands). The presence of the pipe structures itself is not sufficient for determining the current state of a potential reservoir and additionally measures are required evaluate the explorations risks associated with the presented leads. Nevertheless, this study demonstrates the power of using seismically imaged focused fluid conduits as indicators for hydrocarbon systems in poorly explored areas. The close spatial correlation of pipe structures and known hydrocarbon reservoirs in the ESP suggests that mapping these seismic anomalies in high-quality 3D seismic data is an extremely efficient tool to constrain hydrocarbon prospectivity in frontier areas. Obvious targets for a follow-up study with this approach are the conjugate platform areas on the Norwegian Margin on which major fields such as Johan Sverdrup have already been discovered.

ACKNOWLEDGEMENTS

We would like to thank PGS for granting access to the 3D seismic datasets. We would also like to thank the British Oil and Gas Authority for making well data from the study area publically available. Furthermore, we thank the reviewers Daniel Packham and Mads Huuse for improving the quality of this study with their helpful comments. For this study, we used the seismic interpretation software packages Petrel by Schlumberger and Kingdom Suite by IHS. We thank both companies to make their software available for educational purposes.

FIGURES

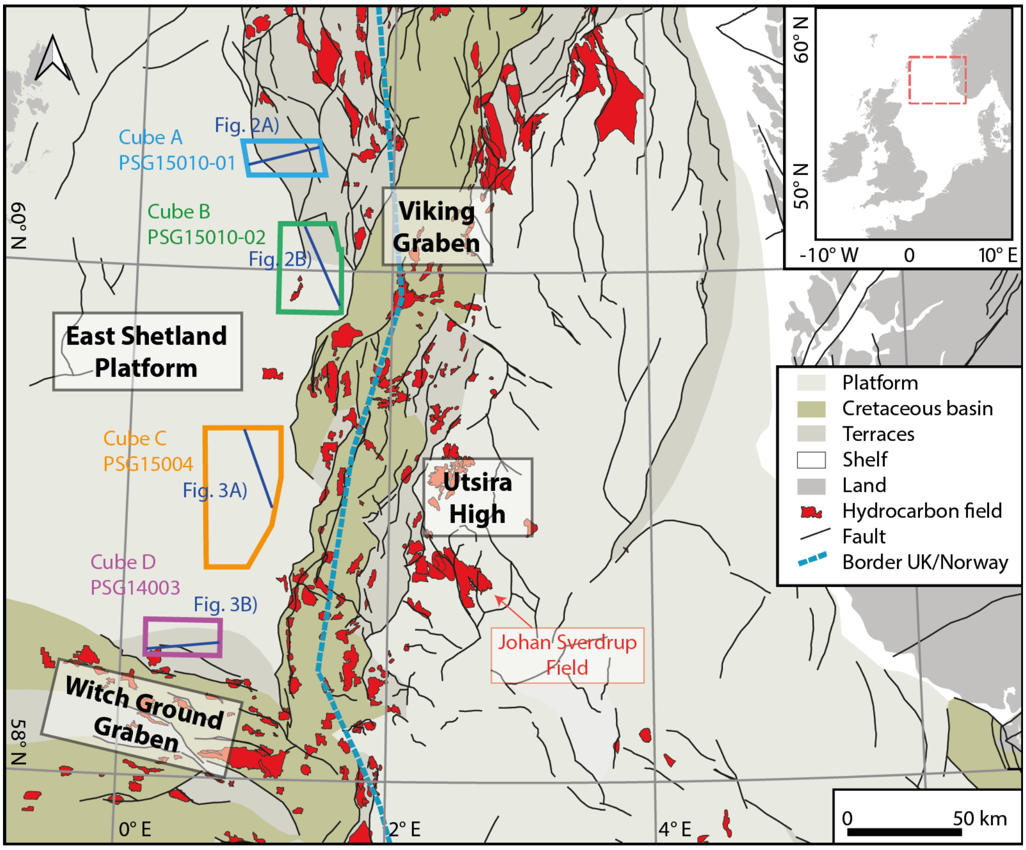

Fig. 1: Map of the Northern North Sea Basin showing the major structural elements, hydrocarbon reservoirs in the Norwegian and British sectors (according to The Norwegian Petroleum Directorate) and the location of the analysed datasets.

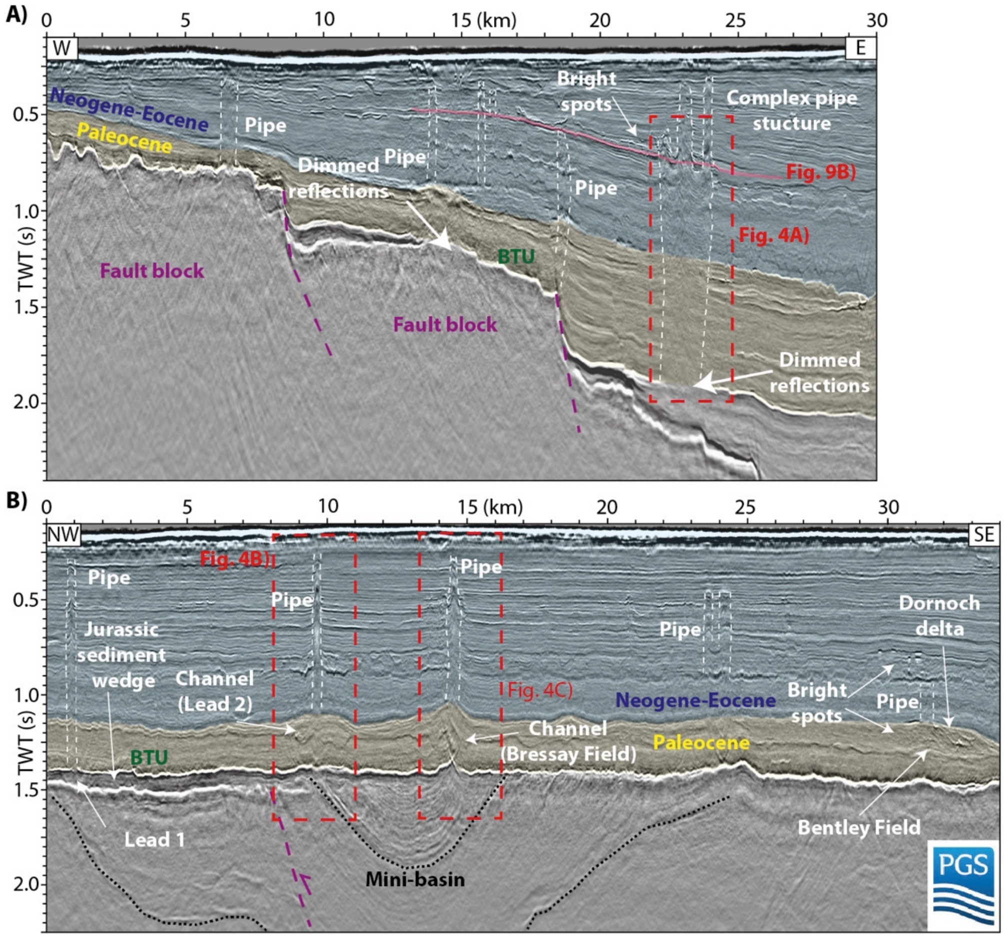

Fig. 2: A) Seismic profile crossing dataset A (PGS15010-01). B) Seismic profile crossing dataset B (PGS15010-02).

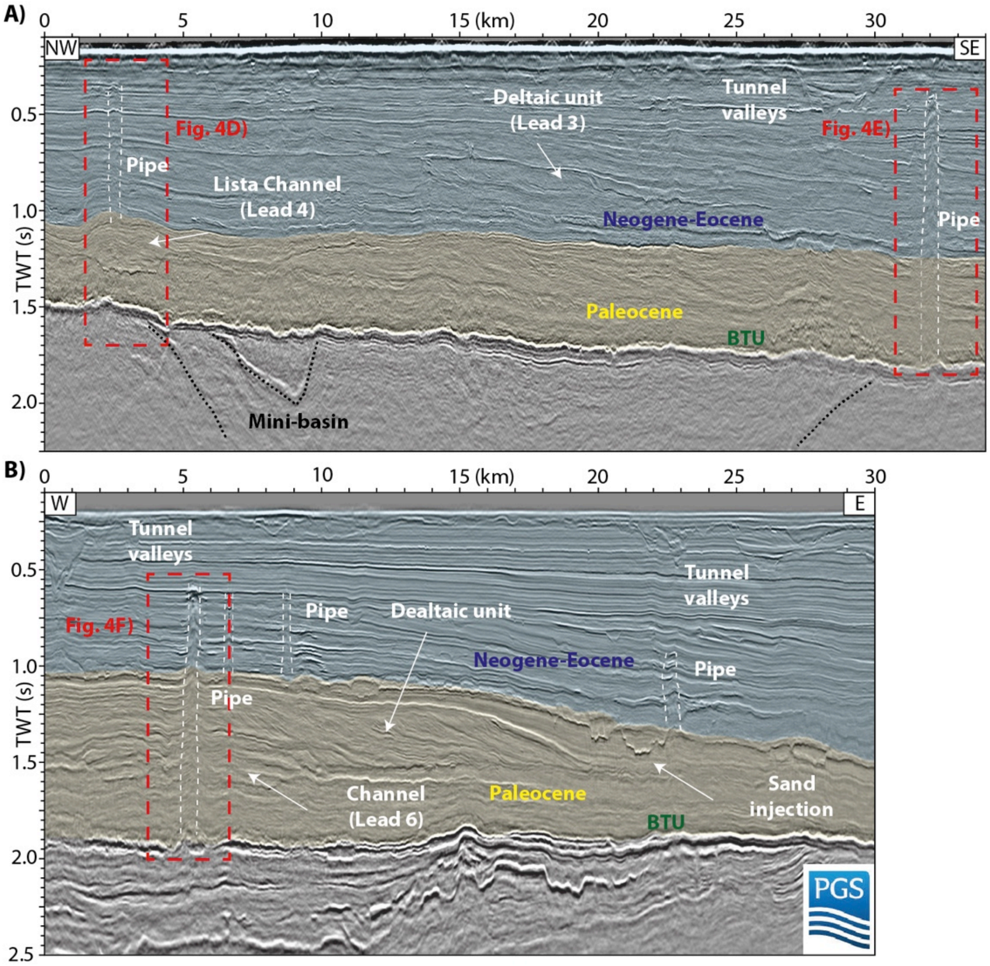

Fig. 3: A) Seismic profile crossing dataset C (PGS15004). B) Seismic profile crossing dataset D (PGS14003).

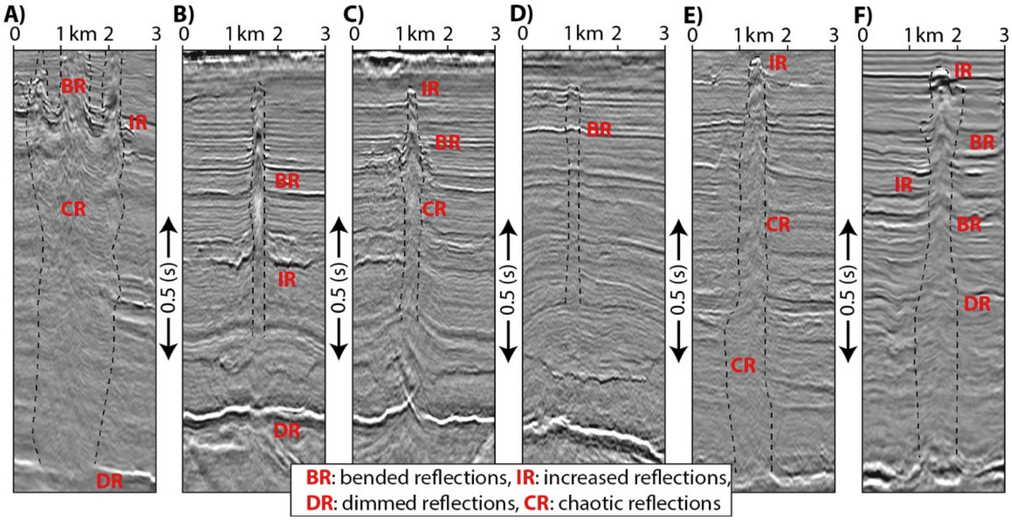

Fig. 4: Seismic examples of pipe structures associated with focused fluid flow.

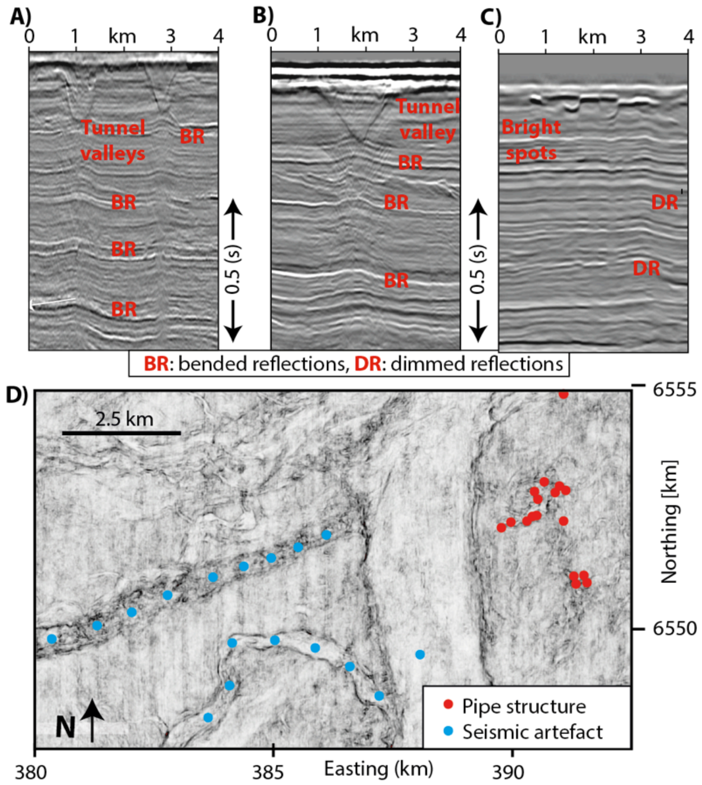

Fig. 5: A-B) Examples of seismic artefacts beneath tunnel valleys. C) Seismic anomaly beneath shallow high amplitude anomaly. D) Variance time slice at 400 ms TWT showing tunnel valleys and seismic anomalies interpreted as artefacts (blue dots) and pipe structures (red dots).

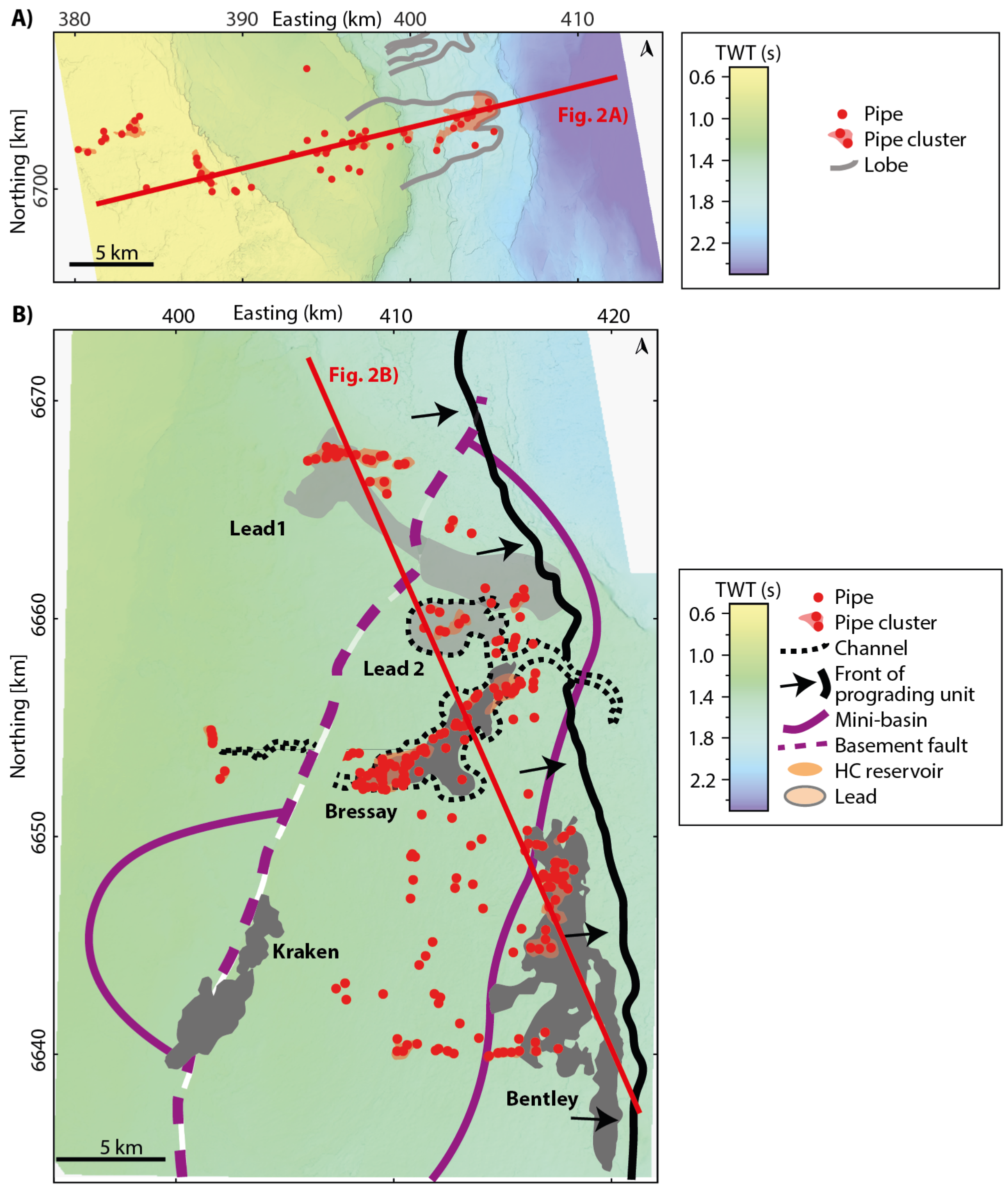

Fig. 6: A) Map showing the distribution of pipe structures in dataset A with major structural and depositional structures affecting fluid flow. B) Map showing the distribution of pipe structures in dataset B with major structural and depositional structures affecting fluid flow, leads and known hydrocarbon fields.

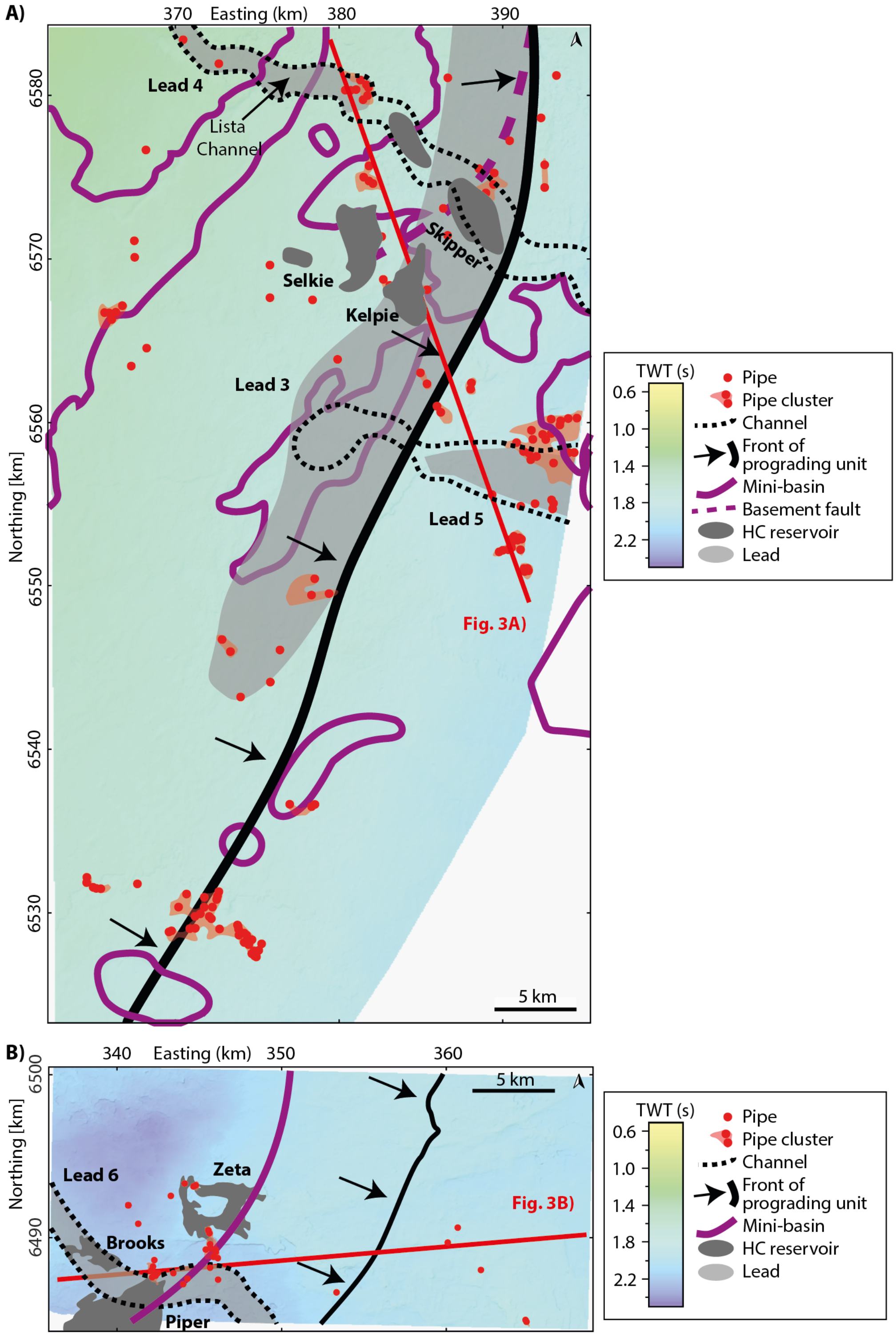

Fig. 7: A) Map showing the distribution of pipe structures in dataset C with major structural and depositional structures affecting fluid flow, leads and known hydrocarbon fields. B) Map showing the distribution of pipe structures in dataset D with major structural and depositional structures affecting fluid flow, leads and known hydrocarbon fields.

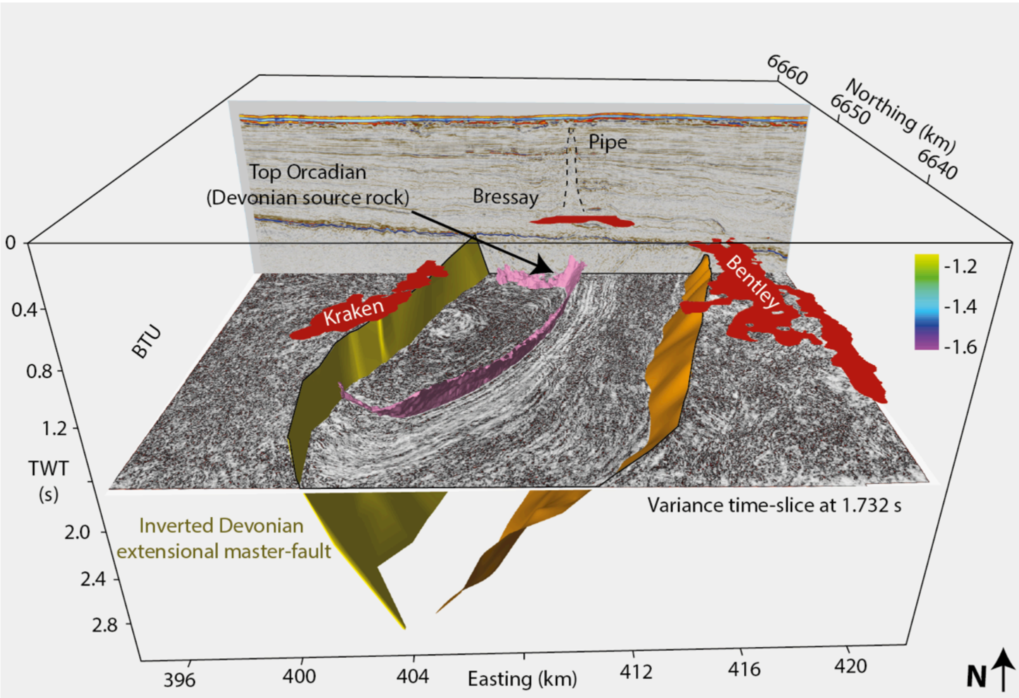

Fig. 8: 3D view on the basin structure in dataset B bound by yellow (inverted extensional fault) and orange horizon. The BTU reflection is cut off in the area of the basin. Pink horizon marks the top of the possible Orcadian source rocks (Patruno and Reid 2017; Patruno et al. 2018) and the red polygons mark the location of hydrocarbon reservoirs.

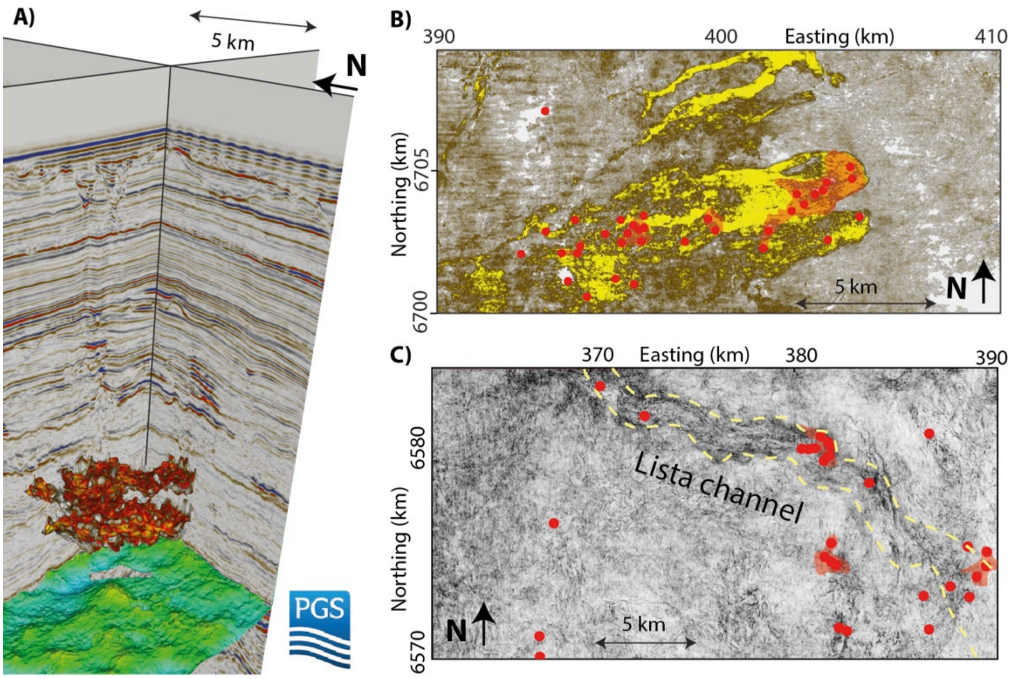

Fig. 9: Examples for refocusing of fluid flow. A) Saucer-shaped sand injections and pipe structures and high amplitude patches rooting at the edge of the sand injection. B) Amplitude map from dataset A showing lobe structures within (likely Oligocene) sediments, which

correlate with pipe structure distribution. C) Variance time slide from dataset C showing the Lista channel with pipe structures.

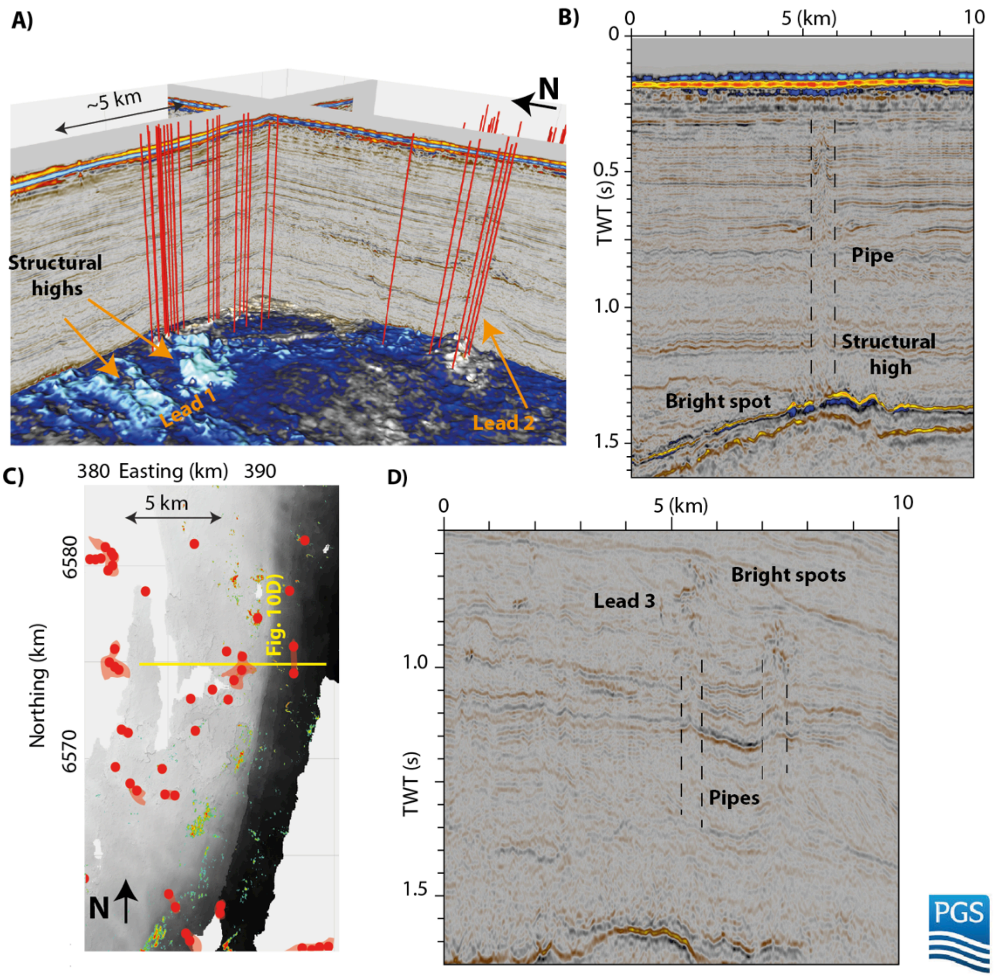

Fig. 10: Examples of leads. A) 3D view on the seismic horizon of the BTU reflection in dataset B showing leads 1 and 2 (c.f. Fig. 2B). B) Seismic profile showing high amplitude reflection above the Jurassic sediment wedge defining Lead 1 and a pipe structure. C) Amplitude map beneath the deltaic unit defining Lead 3 in dataset C (c.f., Fig. 3A). D) Seismic profile showing pipe structures entering Lead 3 and patches of bright spots above.

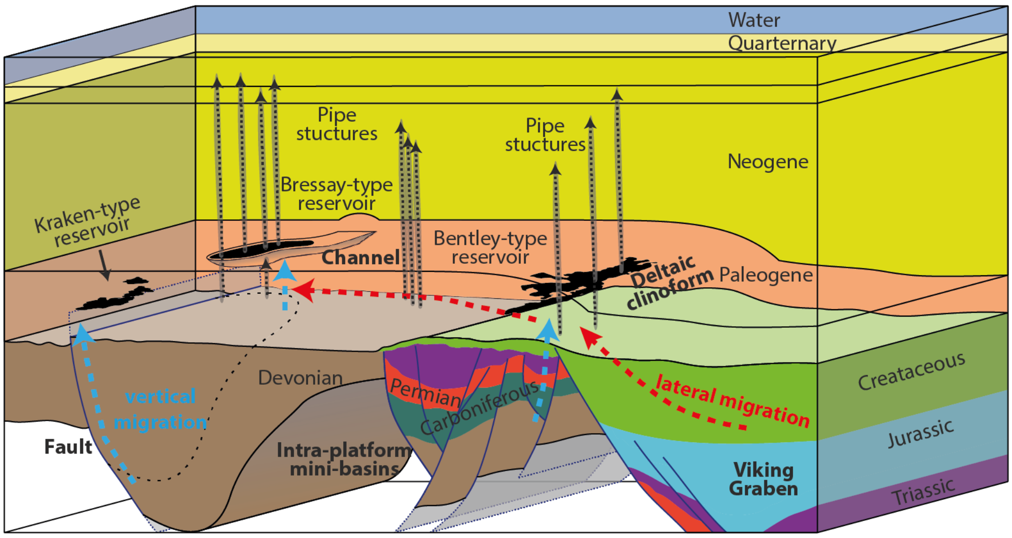

Fig. 11: Generic overview sketch of the of the focused fluid flow system at the eastern margin of the ESP. Arrows indicating potential fluid pathways responsible for charging of Paleocene hydrocarbon reservoirs via lateral migration from the Viking Graben or vertical migration from intra-platform Permo-Triassic mini-basins.

TABLES

Tab. 1: Seismic datasets used in this study with acquisition and processing parameters.

Survey name Survey shortcut	PGS15010-01 **Cube A**	PGS15010-02 **Cube B**	PGS15004 **Cube C**	PGS14003 **Cube D**
Area [km²]	500	1000	1800	500
Area	UKSC East Shetland Platform	UKSC East Shetland Platform	Quad 8, UK	Quad 15, UK
Maximal latitude	N 60° 30′ 35.81″	N 60° 11′ 13.66″	N 59° 22′ 59.49″	N 58° 37′ 25.80″
Minimal latitude	N 60° 22′ 00.70″	N 59° 49′ 47.64″	N 58° 49′ 33.30″	N 58° 28′ 07.67″
Maximal longitude	E 01° 27′ 34.05″	E 01° 36′ 37.78″	E 01° 11′ 11.99″	E 00° 45′ 06.06″
Minimal longitude	E 00° 47′ 32.51″	E 00° 05′ 45.83″	E 00° 34′ 30.58″	E 00° 10′ 26.93″
Survey datum	ED 50	ED 50	ED50	ED50
Projection	UTM 31 N	UTM 31 N	UTM 31 N	UTM 31 N
Sample interval [ms]	2.0	2.0	2.0	2.0
Shot Interval [m]	12.5m-18.75m	12.5m-18.75m	18.75 (Flip/Flop)	18.75 (Flip/Flop)
Source	BOLT 1900-G-Gun II	BOLT 1900-G-Gun II	G-Gun	BOLT 1900LLXT
Volume [CU]	4130-4135	4130-4135	4135	4130
Pressure [PSI]	2000	2000	2000	2000
Airgun Depth [m]	6.0-7.0	6.0-7.0	7.0	7.0
Separation [m]	25-50	25-50	37.5	37.5

Number of Arrays	2	2	2	2
Number of Streamer	10-12	10-12	12	12
Number of Groups	480	480	480	480
Group interval	12.5	12.5	12.5	12.5
Streamer Separation [m]	50-100	50-100	75	75
Streamer depth [m]	15-25	15-25	20-25	20
Streamer length [m]	6000	6000	6000	6000
CDP fold	80	80	80	80
Inline offset [m]	85-160	85-160	160	102
Bin Data [m]	12.5x12.5	12.5x12.5	18.75x12.5	12.5x12.5
Regularization [m]			12.5x12.5	
Migration	Kirchhoff Pre-Stack Time Migration	Kirchhoff Pre-Stack Time Migration	Kirchhoff Pre-Stack Time Migration	Kirchhoff Pre-Stack Depth Migration
Frequency band [Hz]	1 – 95	1- 95	1- 90	1- 85
Dominant frequency [Hz]	30	30	30	40
Vertical resolution above BTU (m)	23	21	23	18

REFERENCES

Andresen, K.J., 2012. Fluid flow features in hydrocarbon plumbing systems: What do they tell us about the basin evolution? Marine Geology, 1–20.

Arntsen, B., Wensaas, L., Løseth, H., Hermanrud, C., 2007. Seismic modeling of gas chimneys. Geophysics 72, 251–259.

Badley, M. E., Price, J. D., Dahl, C. R., & Agdestein, T., 1988. The structural evolution of the northern Viking Graben and its bearing upon extensional modes of basin formation. Journal of the Geological Society, 145(3), 455-472.

Berndt, C., 2005. Focused fluid flow in passive continental margins. Philosophical Transactions of the Royal Society A: Mathematical, Physical and Engineering Sciences 363, 2855–2871.

Böttner, C. , Berndt, C. , Reinardy, B. T. I., Geersen, J. , Karstens, J., Bull, J. M. , Callow, B. J. , Lichtschlag, A. , Schmidt, M. , Elger, J. , Schramm, B. und Haeckel, M. (2019) Pockmarks in the Witch Ground Basin, central North Sea. Geochemistry, Geophysics, Geosystems .

Blystad, P., Brekke, H., Færseth, R.B., Larsen, B.T., Skogseid, J. & Tørudbakken, B., 1995. Structural Elements of the Norwegian Continental Shelf. Part II: The Norwegian Sea Region. Norwegian Petroleum DirectoratebBulletin, 8.

Brown, S., 1990. Jurassic. In:Glennie, K.W. (ed.) Introduction to the Petroleum Geology of the North Sea. Blackwell Scientific, Oxford, 219-254.

Cartwright, J. A., and Santamarina, C. (2015). Seismic characteristics of fluid escape pipes in sedimentary basins: Implications for pipe genesis. Marine And Petroleum Geology, 65 (2015), 126 - 140. doi:10.1016/j.marpetgeo.2015.03.023

Cartwright, J., Huuse, M., Aplin, A., 2007. Seal bypass systems. AAPG Bulletin 91, 1141–1166.

Cathles, L.M., Su, Z., Chen, D., 2010. The physics of gas chimney and pockmark formation, with implications for assessment of seafloor hazards and gas sequestration. Marine and Petroleum Geology 27,

Clayton, C.J., Hay, S.J., 1992. Gas migration mechanisms from accumulation to surface. Bulletin of the Geological Society of Denmark 41, 12-23.

Cornford, C., 2009. Source rocks and hydrocarbons of the North Sea. In: Glennie, K.W. (ed.) *Petroleum geology of the North Sea: Basic concepts and recent advances*, 376-462.

Davies, R. J., O'Donnell, D., Bentham, P. N., Gibson, J. P. C., Curry, M. R., Dunay, R. E., & Maynard, J. R., 1999. The origin and genesis of major Jurassic unconformities within the triple junction area of the North Sea, UK. In Geological Society, London, Petroleum Geology Conference series (Vol. 5, No. 1, pp. 117-131). Geological Society of London.

Duncan, W. I., & Buxton, N. W. K., 1995. New evidence for evaporitic Middle Devonian lacustrine sediments with hydrocarbon source potential on the East Shetland Platform, North Sea. Journal of the Geological Society, 152(2), 251-258.

Fyfe, J. A., Abbotts, I., & Crosby, A., 1981. The subcrop of the mid-Mesozoic unconformity in the UK area. Petroleum Geology of the Continental Shelf of North-West Europe. Institute of Petroleum, London, 236, 244.

Gabrielsen, R. H., Foerseth, R., Hamar, G., & Rønnevik, H., 1984. Nomenclature of the main structural features on the Norwegian Continental Shelf north of the 62nd parallel. In Petroleum Geology of the North European Margin (pp. 41-60). Springer, Dordrecht.

Gabrielsen, R. H., Færseth, R. B., Steel, R. J., Idil, S., Kløvjan, O. S., Blundell, D. J., & Gibbs, A. D., 1990. Architectural styles of basin fill in the northern Viking Graben. Tectonic Evolution of the North Sea Rifts. Clarendon Press, Oxford, 158, 179.

Granli, J.R., Arntsen, B., Sollid, A., Hilde, E., 1999. Imaging through gas-filled sediments using marine shear-wave data. Geophysics 64, 668–677.

Hancock, J.M., 1990. Cretaceous. In: Glennie, K.W. (ed) Introduction to the Petroleum Geology of the North Sea. Blackwell Scientific, Oxford, 255-272.

Harker, S. D., Green, S. C. H., & Romani, R. S., 1991. The Claymore Field, Block 14/19, UK North Sea. *Geological Society, London, Memoirs*, *14*(1), 269-278.

Haszeldine, R. S., 2009. Carbon capture and storage: how green can black be? Science, 325(5948), 1647-1652.

Heggland, R., 2005. Using gas chimneys in seal integrity analysis: A discussion based on case histories, in P. BoultandJ. Kaldi, eds.,Evaluating fault and cap rock seals: AAPG Hedberg Series, no. 2, p. 237-245. Evaluating fault and cap rock seals, (2), 237.

Hill, P. J., & Smith, G., 1979. Geological aspects of the drilling of the Buchan field. In *Offshore Europe*. Society of Petroleum Engineers.

Hillman, J. I., Burwicz, E., Zander, T., Bialas, J., Klaucke, I., Feldman, H., ... & Awwiller, D., 2018. Investigating a gas hydrate system in apparent disequilibrium in the Danube Fan, Black Sea. Earth and Planetary Science Letters, 502, 1-11.

Hovland, M., Sommerville, J.H., 1985. Characteristics of two natural gas seepages in the North Sea. Marine and Petroleum Geology 2, 319–326.

Hseinat, Al, M., Hübscher, C., 2014. Ice-load induced tectonics controlled tunnel valley evolution - instances from the southwestern Baltic Sea. Quaternary Science Reviews 97, 121–135. doi:10.1016/j.quascirev.2014.05.011

Hubbert, M.K., Willis, D.G., 1957. Mechanic of hydraulic fracturing. Transactions of Society of Petroleum Engineers of AIME, 1957, v. 210, p. 153-168.

Huuse, M., & Mickelson, M., 2004. Eocene sandstone intrusions in the Tampen Spur area (Norwegian North Sea Quad 34) imaged by 3D seismic data. Marine and Petroleum Geology, 21(2), 141-155.

IGI, 2017. Source rock potential of the East Shetland Platform area. Report for the UK Oil and Gas Authority.

Johnson, 1975. The base Cretaceous: a discussion. In: Woodland, A.W. (ed.) Petroleum and the Continental Shelf of the North West Europe. John Wiley & Sons, New York, 1, 389-402.

Judd, A., & Hovland, M., 2007. Seabed fluid flow: the impact on geology, biology and the marine environment. Cambridge University Press.

Karstens, J., & Berndt, C., 2015. Seismic chimneys in the Southern Viking Graben – Implications for palaeo fluid migration and overpressure evolution. Earth and Planetary Science Letters, 412(0), 88–100. doi:http://dx.doi.org/10.1016/j.epsl.2014.12.017

Karstens, J., Ahmed, W., Berndt, C., & Class, H., 2017. Focused fluid flow and the sub-seabed storage of CO2: Evaluating the leakage potential of seismic chimney structures for the Sleipner CO2 storage operation. Marine and Petroleum Geology, 88, 81-93.

Karstens, J., Haflidason, H., Becker, L. W., Berndt, C., Rüpke, L., Planke, S., ... & Mienert, J. (2018). Glacigenic sedimentation pulses triggered post-glacial gas hydrate dissociation. Nature communications, 9(1), 635.

Kristensen, T.B., Huuse, M., 2012. Multistage erosion and infill of buried Pleistocene tunnel valleys and associated seismic velocity effects. Geological Society, London, Special Publications 368, 159–172. doi:10.1144/SP368.15

Kyrkjebø, R., Gabrielsen, R. H., & Faleide, J. I., 2004. Unconformities related to the Jurassic–Cretaceous synrift–post-rift transition of the northern North Sea. Journal of the Geological Society, 161(1), 1-17.

Leifer, I., &Judd, A., 2015. The UK22/4b blowout 20 years on: Investigations of continuing methane emissions from sub-seabed to the atmosphere in a North Sea context. Marine and Petroleum Geology, 68, 706-717.

Lønøy, A., Akselsen, J., and Rønning, K., 1986. Diagenesis of a deeply buried sandstone reservoir: Hild Field, Northern North Sea. Clay Minerals, 21(4), 497-511.

Løseth, H., Gading, M., Wensaas, L., 2009. Hydrocarbon leakage interpreted on seismic data. Marine and Petroleum Geology 26, 1304–1319.

Løseth, H.,Wensaas, L., Arntsen, B., Hanken, N.-M., Basire, C., Graue, K., 2011. 1000 m long gas blow-out pipes. Marine and Petroleum Geology 28, 1047–1060.

Maher, C. E. (1981). Development geology of the Piper Oilfield. *Ocean Management*, *7*(1-4), 133-165.

Mark, D. F., Green, P. F., Parnell, J., Kelley, S. P., Lee, M. R., & Sherlock, S. C., 2008. Late Palaeozoic hydrocarbon migration through the Clair field, West of Shetland, UK Atlantic margin. *Geochimica et Cosmochimica Acta*, *72*(10), 2510-2533.

Marshall, J. E. A., & Hewett, A. J., 2003. Devonian. In: Evans, D., Graham, C., Armour, A. & Bathurst, P. (eds) The Millenium Atlas: Petroleum Geology, Geological Society of London.

Marshall, J. E. A., 1998. The recognition of multiple hydrocarbon generation episodes: an example from Devonian lacustrine sedimentary rocks in the Inner Moray Firth, Scotland. *Journal of the Geological Society*, *155*(2), 335-352.

Mazzini, A., Svensen, H. H., Planke, S., Forsberg, C. F., &Tjelta, T. I., 2016. Pockmarks and methanogenic carbonates above the giant Troll gas field in the Norwegian North Sea. Marine Geology, 373, 26-38.

Monaghan, A. A., Johnson, K., Arsenikos, S., Callaghan, E., Fellgett, M., Hannis, S., Henderson, A.; Leslie, G.; Kearsey, T.; Kim, A.; Kimbell, G.; Quinn, M.; McLean, W.; Millward, D.; Sankey, M.; Smith, N.; Uguna, C.; Vane, C.; Vincent, C.; Williamson, P, 2016. Palaeozoic Petroleum Systems of the Orcadian Basin to Forth Approaches, Quadrants 6-21, UK. British Geological Survey, Energy and Marine Geoscience Programme Commissioned Report CR/16/038N British Geological Survey. http://nora.nerc.ac.uk/id/eprint/516781/

Moss, J. L., & Cartwright, J., 2010. 3D seismicexpressionof km-scale fluid escapepipesfrom offshore Namibia. Basin Research, 22(4), 481-501.

Nøttvedt, A., Gabrielsen, R. H., & Steel, R. J., 1995. Tectonostratigraphy and sedimentary architecture of rift basins, with reference to the northern North Sea. Marine and Petroleum Geology, 12(8), 881-901.

Ottesen, D., Dowdeswell, J. A., Rise, L., & Bugge, T., 2012. Large-scale development of the mid-Norwegian shelf over the last three million years and potential for hydrocarbon reservoirs in glacial sediments. Geological Society, London, Special Publications, 368(1), 53-73.

Ottesen, D., Dowdeswell, J. A., & Bugge, T., 2014. Morphology, sedimentary infill and depositional environments of the Early Quaternary North Sea Basin (56–62 N). Marine and Petroleum Geology, 56, 123-146.

Patruno, S., & Reid, W., 2016a. New plays on the Greater East Shetland Platform (UKCS Quadrants 3, 8–9, 14–16)–part 1: Regional setting and a working petroleum system. *first break*, *34*(12), 33-43.

Patruno, S., & Reid, W., 2016b. The East Shetland Platform and Mid North Sea High. GeoExpro, 13, June 2016, https://www.geoexpro.com/articles/2016/07/the-east-shetland-platform-and-mid-north-sea-high

Patruno, S., & Reid, W., 2017. New plays on the greater east Shetland platform (UKCS quadrants 3, 8–9, 14–16)—Part 2: Newly reported Permo-Triassic intra-platform basins and their influence on the Devonian-Paleogene prospectivity of the area. First Break, 35(1), 59-69.

Patruno, S., Helland-Hansen, W., 2018. Clinoform systems: Review and dynamic classification scheme for shorelines, subaqueous deltas, shelf edges and continental margins. Earth-Science Reviews, 185, 202-233.

Patruno, S., Reid, W., Jackson, C. A-L., 2018. New insights into the unexploited reservoir potential of the Mid North Sea High (UKCS Quadrants 35-38, 41-43): a newly-described intra Zechstein sulphate-carbonate platform complex. In: Bowman, M. & Levell, B. (eds), Petroleum Geology of Northwest

Europe: 50 Years of Learning – Proceedings of the 8th Petroleum Geology Conference. The Geological Society, London, United Kingdom, v. 8, p. 87–124.

Patruno, S., Reid, W., Berndt, C., Feuilleaubois, L., 2019. Polyphase tectonic inversion and its role in controlling hydrocarbon prospectivity in the Greater East Shetland Platform and Mid North Sea High, offshore UK. In: A.A. Monaghan, J.R. Underhill, A.J. Hewett, J.E.A. Marshall (Eds.), Palaeozoic Plays of NW Europe, The Geological Society, Special Publications, London, United Kingdom, Vol. 471, p. 177-235.

Patruno, S., Scisciani, V., Pellegrini, C., Helland-Hansen, W., Reid, W., D'Intino, D., in press. Climbing clinoforms of the Mid North Sea High (lower Pleistocene Eridanos Delta): when sediment supply overwhelms accommodation. Accepted for publication in Basin Research, March 2019.

Pegrum, R. M., & Spencer, A. M., 1990. Hydrocarbon plays in the northern North Sea. *Geological Society, London, Special Publications*, *50*(1), 441-470.

Plaza-Faverola, A., Bünz, S., & Mienert, J. (2011). Repeated fluid expulsion through sub-seabed chimneys offshore Norway in response to glacial cycles. Earth and Planetary Science Letters, 305(3-4), 297–308.

Rawson, P. F., & Riley, L. A., 1982. Latest Jurassic-Early Cretaceous Events and the. AAPG Bulletin, 66(12), 2628-2648.

Reinardy, B. T. I., Hjelstuen, B. O., Sejrup, H. P., Augedal, H., Jørstad, A. (2017). Late Pliocene-Pleistocene environments and glacial history of the northern North Sea. Quaternary Science Reviews, 158, 107 – 126. doi: 10.1016/j.quascirev.2016.12.022

Relinquishment Report for License P976

Relinquishment report for seaward production licence P1946

Rønnevik, H. C., Van Den Bosch, W., & Bandlien, E. H., 1975. A proposed nomenclature for the main structural features in the Norwegian North Sea. In: Finstad, KG & Selley, RC (eds): Jurassic Northern North Sea Symposium, Stavanger (pp. 28-30).

Scisciani, V., Patruno, S., Tavarnelli, E., Calamita, F., Pace, P., Iacopini, D., in press. Multi-phase reactivations and inversions of Paleozoic-Mesozoic extensional basins during the Wilson Cycle: case studies from the North Sea (UK) and Northern Apennines (Italy). In: Wilson, R.W., Houseman, G.A., McCaffrey, K.J.W., Doré A.G. and Buiter, S.J.H. (Eds.), Fifty Years of the Wilson Cycle Concept in Plate Tectonics. Geological Society Special Publications, The Geological Society, London, United Kingdom, v. 470, p. xxxx.

Sejrup, H. P., Bentley, M., Hjelstuen, B. O., & Ó Cofaigh, C., 2018. Geological evolution and processes of the glaciated North Atlantic margins. Marine Geology, 402, 1-4.

Szarawarska, E., Huuse, M., Hurst, A., De Boer, W., Lu, L., Molyneux, S., & Rawlinson, P., 2010. Three-dimensional seismic characterisation of large-scale sandstone intrusions in the lower Palaeogene of the North Sea: completely injected vs. in situ remobilised sandbodies. Basin Research, 22(4), 517-532.

Turner, C.C., Cronin, B.T., Riley, L.A., Patruno, S., Reid, W.T.L.R., Hoth, S., Knaust, D., Allerton, S., Jones, M.A. and Jackson, C.A-L., 2018. The South Viking Graben: Overview of Upper Jurassic rift geometry, biostratigraphy and extent of Brae Play submarine fan systems, in: Colin C. Turner and Bryan T. Cronin (Eds.), Rift-related coarse-grained submarine fan reservoirs; the Brae Play, South

Viking Graben, North Sea: American Association of Petroleum Geologists (AAPG) Memoir 115, p. 9-38.

Underhill, J. R., & Partington, M. A. 1993. Jurassic thermal doming and deflation in the North Sea: implications of the sequence stratigraphic evidence. In *Geological Society, London, Petroleum Geology Conference series* (Vol. 4, No. 1, pp. 337-345). Geological Society of London.

Underhill, J. R., 2001. Controls on the genesis and prospectivity of Paleogenepalaeogeomorphic traps, East Shetland Platform, UK North Sea. Marine and Petroleum Geology, 18(2), 259-281.

Vane, C. H., Uguna, C., Kim, A. W., & Monaghan, A. A., 2016. Organic Geochemistry of Palaeozoic Source Rocks, Orcadian Study Area, North Sea, UK. British Geological Survey Commissioned Report CR/16/037. http://nora.nerc.ac.uk/id/eprint/516754

White, J. E., 1975. Computed seismic speeds and attenuation in rocks with partial gas saturation. Geophysics, 40(2), 224-232.

Whitehead, M., & Pinnock, S. J., 1991. The Highlander Field, Block 14/20b, UK North Sea. *Geological Society, London, Memoirs*, *14*(1), 323-329.

Yaliz, A., 1991. The Crawford Field, Block 9/28a, UK North Sea. *Geological Society, London, Memoirs*, *14*(1), 287-294.

Ziegler, P. A., 1975a. North Sea basin history in the tectonic framework of north-western Europe. In: Woodland, A.W. (ed) Proceedings of the 4th Conference Petroleum Geology, Petroleum and the continental shelf of North-West Europe, 1, 131-149.

Ziegler, W. H. 1975b. Outline of the geological history of the North Sea. In: Woodland, A.W. (ed.) Proceedings of the 4th Conference Petroleum Geology, Petroleum and the Continental Shelf of North-West Europe. John Wiley & Sons, New York, 1, 165–187.

Ziegler, P. A., 1992. European Cenozoic rift system. Tectonophysics, 208(1), 91–111.